THE JOURNAL OF BIOLOGICAL CHEMISTRY VOL. 285, NO. 7, pp. 4883–4895, February 12, 2010

Phosphorylation of VACM-1/Cul5 by Protein Kinase A Regulates Its Neddylation and Antiproliferative Effect*

Received for publication, November 14, 2009 Published, JBC Papers in Press, November 16, 2009, DOI 10.1074/jbc.M109.085225

Shirley E. Bradley[1], Alyssa E. Johnson[1], Isabelle P. Le, Elizabeth Oosterhouse, Michael P. Hledin, Gabriel A. Marquez, and Maria Burnatowska-Hledin[2]

From the Departments of Biology and Chemistry, Hope College, Holland, Michigan 49422-9000

Expression of the *VACM-1*/*cul5* gene in endothelial and in cancer cell lines *in vitro* inhibits cellular proliferation and decreases phosphorylation of MAPK. Structure-function analysis of the VACM-1 protein sequence identified consensus sites specific for phosphorylation by protein kinases A and C (PKA and PKC) and a Nedd8 protein modification site. Mutations at the PKA-specific site in VACM-1/Cul5 (^{S730A}VACM-1) sequence resulted in increased cellular growth and the appearance of a Nedd8-modified VACM-1/Cul5. The aim of this study was to examine if PKA-dependent phosphorylation of VACM-1/Cul5 controls its neddylation status, phosphorylation by PKC, and ultimately growth. Our results indicate that *in vitro* transfection of rat adrenal medullary endothelial cells with anti-*VACM-1*-specific small interfering RNA oligonucleotides decreases endogenous VACM-1 protein concentration and increases cell growth. Western blot analysis of cell lysates immunoprecipitated with an antibody directed against a PKA-specific phosphorylation site and probed with anti-VACM-1-specific antibody showed that PKA-dependent phosphorylation of VACM-1 protein was decreased in cells transfected with ^{S730A}*VACM-1* cDNA when compared with the cytomegalovirus-transfected cells. This change was associated with increased modification of VACM-1 protein by Nedd8. Induction of PKA activity with forskolin reduced modification of VACM-1 protein by Nedd8. Finally, rat adrenal medullary endothelial cells transfected with ^{S730A}*VACM-1*/*cul5* cDNA and treated with phorbol 12-myristate 13-acetate (10 and 100 nM) to induce PKC activity grew significantly faster than the control cells. These results suggest that the antiproliferative effect of VACM-1/Cul5 is dependent on its posttranslational modifications and will help in the design of new anticancer therapeutics that target the Nedd8 pathway.

VACM-1 (vasopressin-activated calcium-mobilizing) protein (1), now identified as a *cul5* gene product (2–4), is a 780-amino acid protein with a calculated M_r of 91 kDa. Transfection of various cell lines with *VACM-1*/*cul5* cDNA attenuates cellular growth by a mechanism that involves inhibition of cAMP production, decreased phosphorylation of MAPK,[3] and a decrease in nuclear localization of early growth response gene (*egr-1*) product (5–7). *In vivo*, VACM-1/Cul5 protein expression is specific to established endothelial cells (8) but is absent in sprouting capillaries (9), suggesting its involvement in the regulation of endothelium-specific growth. Interestingly, the human homolog of VACM-1 differs only in six amino acids from the rabbit VACM-1 and has been proposed to be a candidate for a tumor suppressor (2). Although expression of *VACM-1*/*cul5* cDNA in a cancer-derived cell line, T47D, decreased nuclear concentration of estrogen receptor, ERα, and inhibited cellular growth (6), the precise mechanism by which VACM-1/Cul5 may regulate cell growth is not known. Like other cullins, however, VACM-1/Cul5 may serve as scaffold protein that allows the assembly of E3 ubiquitin ligase complexes involved in protein ubiquitination and, ultimately, degradation (10).

Proteasome-dependent protein degradation involves three ligases (E1–E3), which promote activation (E1), conjugation (E2), and ligation (E3) of ubiquitin to a substrate marked for degradation (11, 12). The E3 ligases are further divided into three groups based on their structure and substrate recognition (13–15). The most abundant group of the E3 ligases is characterized by the presence of a RING (really interesting new gene) finger domain and uses cullin family members to recognize specific motifs on their substrates (16). The numerous E3 ligase complexes can be further regulated by the posttranslational modifications of their components (11). For example, activation of E3 ubiquitin ligase *Itch* is regulated by phosphorylation-induced conformational changes (17, 18), and COP1 E3 ligase, which affects p53 ubiquitination, is phosphorylated by the ATM kinase (19). The specificity of the ubiquitin-proteasome degradation system is further controlled through modification of cullins by Nedd8 protein, which shares 58% identity and 79% similarity with ubiquitin (20–22). It is now proposed that cullins must be neddylated and form heterodimers to be an active component of the E3 ligase system (14). Conjugation of Nedd8 to Cul1 enhances the ability of the complex to promote ubiquitin polymerization and is essential for proteolytic targeting of

* This work was supported, in whole or in part, by National Institutes of Health (NIH) Grant RO1DK47199 and NIH, NCI, Grant R15CA104014. This work was also supported by a Beckman Foundation Award (to S. E. B.), a Research Experience Across Cultures at Hope program award to high school student (G. A. M.), and a Merck/American Association for the Advancement of Science Undergraduate Science Research Program Award from the Merck Institute for Science Education.

[1] Both of these authors contributed equally to this work.

[2] To whom correspondence should be addressed: Dept. of Biology, Science Center, Hope College, Holland, Michigan 49422-9000. Tel.: 616-395-7764; Fax: 616-395-7125; E-mail: hledin@hope.edu.

[3] The abbreviations used are: MAPK, mitogen-activated protein kinase; PKA, protein kinase A; PKC, protein kinase C; PMA, phorbol 12-myristate 13-acetate; FSK, forskolin; Ab, antibody; RAMEC, rat adrenal medullary endothelial cell(s); PBS, phosphate-buffered saline; BSA, bovine serum albumin; DAPI, 4′,6-diamidino-2-phenylindole; CMV, cytomegalovirus; siRNA, small interfering RNA; GAPDH, glyceraldehyde-3-phosphate dehydrogenase.

$p27^{Kip1}$ (10, 22–24). Loss of the Nedd8 system, on the other hand, leads to the dysfunction of tumor suppression by von Hippel-Linden (25) and compromises Cul1-dependent regulation of eye development in *Drosophila* (26), whereas in mice it is essential for cell cycle progression (27). In *Caenorhabditis elegans* development, neddylated Cul1 targets katanin, a microtubule-severing complex, and thus acts as a negative regulator of contractility and cytokinesis (28, 29). Whether modification of cullins by Nedd8 is dependent on their phosphorylation has not been reported.

Analysis of VACM-1/Cul5 protein structure revealed a putative modification sequence for Nedd8 at Lys-724, a protein kinase A (PKA) phosphorylation sequence at Ser-730 and Thr-426, and 15 putative protein kinase C (PKC)-dependent phosphorylation sites (5). The expression of a VACM-1 mutant where Ser-730 has been changed to Ala (^{S730A}*VACM-1*) significantly increased cellular growth and created a dominant negative phenotype (5). Further, overexpression of the mutant in rat adrenal medullary endothelial cells (RAMEC) converted cells to the angiogenic phenotype when grown on a Matrigel® support (9). These results suggested, therefore, that cellular localization and the biological activity of VACM-1/Cul5 protein may depend on its posttranslational modification status by PKA.

The ^{S730A}VACM-1 mutant gives us a powerful tool to determine how PKA-specific phosphorylation induces modification of VACM-1 by Nedd8 and to elucidate the mechanism of phenotype reversal when expressed in endothelial cells *in vitro* (5). This approach has been used by others to discover the mechanism by which PKA activity controls localization and activity of proteins that regulate cell growth and angiogenesis (30–33). For example, PKA-dependent phosphorylation of an oncogene, Gli, increased its nuclear localization (32), whereas phosphorylation of a receptor, GRK2, recruited the protein to the cell membrane (33). Because E3 ligases determine the specificity of the substrates being targeted for degradation, proteasome inhibitors are now marketed as drugs (15). Consequently, identifying VACM-1/Cul5 as a component of the vasculature-specific E3 ligase and determining how neddylation and/or phosphorylation affect its localization and biological activity may be important in identifying specific targets for drugs to control cell growth and angiogenesis.

In this study, we report several new findings that will help elucidate the mechanism of VACM-1/Cul5-dependent cell growth. First, using siRNA oligonucleotides against VACM-1 mRNA, we confirmed the antiproliferative effects of VACM-1/Cul5. Second, we demonstrated that cellular localization of VACM-1/Cul5 proteins may be controlled by its posttranslational modifications. Third, we showed that the expression of ^{S730A}*VACM-1* cDNA, which lacks the PKA-specific phosphorylation site, leads to increased neddylation of VACM-1. Finally, we found that PKC-induced cell proliferation is significantly higher in cells transfected with ^{S730A}*VACM-1* cDNA when compared with the control group. Together, these results suggest that preferential phosphorylation of VACM-1/Cul5 protein by these protein kinases regulates its modification by Nedd8 and may allow for the selective regulation of different cellular pathways (5, 6, 9).

EXPERIMENTAL PROCEDURES

Materials—All tissue culture media and reagents were purchased from Invitrogen. *VACM-1* cDNA was subcloned into the pBK-CMV vector as described previously (34). *VACM-1*/*cul5*-specific siRNAs were purchased from Ambion (Applied Biosystems Inc., Austin, TX). Phorbol 12-myristate 13-acetate (PMA) (catalog number P8139) and Gö6983 (catalog number G1918) were from Sigma. Forskolin (FSK) was purchased from MP Biomedicals (Solon, OH). Polyclonal anti-Nedd8 antibody was from Abcam and monoclonal anti-Nedd8 Ab was purchased from Sigma-Aldrich (St. Louis, MO).

Site-directed Mutagenesis—Site-directed mutagenesis was performed using the QuikChange™ site-directed mutagenesis kit from Stratagene (La Jolla, CA). The mutagenesis primers were synthesized by Sigma-Genosys Inc. (Woodland, TX). To confirm the mutation site, sequencing was performed by Macromolecular Resources (Colorado State University, Ft. Collins, CO) as described previously (5).

Tissue Culture—RAMEC (35) were grown in low glucose Dulbecco's modified Eagle's medium supplemented with 2% fetal bovine serum, 7% horse serum, 89.6 units/ml penicillin, and 89.6 μg/ml streptomycin at 37 °C under a water-saturated 5% CO_2 atmosphere as described previously (36). All cell lines were plated at a density of $6-8 \times 10^5$ cells/100-mm plate and cultured for 24 h before transfection. Cells were transfected with 5 μg of *VACM-1* cDNA (or ^{S730A}*VACM-1* cDNA) per 100-mm culture dish using the FuGENE-6® (Roche Applied Science) (9) or with the Mirus reagent (Mirus, Madison, WI) as described by the manufacturers. After 24 h, cells were split and incubated with fresh medium containing 600 μg/ml G418 (Invitrogen). The medium was changed every 3 days. 2–3 weeks after transfection, G418-resistant cells were harvested and transferred into 6-well plates containing selective medium (250 μg/ml G418) (5).

Immunostaining—Affinity-purified rabbit polyclonal antibody directed against the N terminus (Ab-A) of VACM-1 protein (1, 8) were used to stain cells by indirect immunofluorescence. Cells grown on coverslips were fixed in 3% paraformaldehyde (in 1× PBS, pH 7.4) for 20 min, washed in PBS, permeabilized with 5% Tween 20 solution for 20 min, washed with PBS, 2% BSA, and incubated for 2 h with a 1:20 dilution of Ab-A or with Ab-A preabsorbed with 10 μM peptide A identical in sequence to the N-terminal sequence of VACM-1. Antibodies were diluted in PBS containing 0.1% BSA (PBS/BSA). Cells probed with anti-Nedd8 (Alexis Co.) antibody were treated similarly and exposed to the antibody for 1.5 h. The primary antibodies were detected by incubating cells in the presence of a 1:40 dilution of either fluorescein isothiocyanate-conjugated goat anti-rabbit IgG or Texas Red-conjugated anti-rabbit Ab (Vector Laboratories Inc., Burlingame, CA) in 1× PBS, 2% BSA for 1 h. The slides were washed with 1× PBS with 0.2% BSA, mounted with Vectashield® mounting medium, and viewed by epifluorescence microscopy (Eclipse E600, Nikon) equipped with a Spot camera (Diagnostic Instruments, Sterling Heights, MI). The nuclear staining was achieved by DAPI found in the Vectashield® mounting medium (Vector Laboratories Inc., Burlingame, CA). The relative expression of specific pro-

teins was calculated using the NIH Image program (available on the World Wide Web).

Cellular Proliferation Analysis—RAMEC transfected with *VACM-1* cDNA, ^{S730A}*VACM-1* cDNA, and CMV vector were seeded in 100-mm plates at equal densities (2×10^4 cells/ml), harvested at specified time points, and counted in a hemacytometer. Alternatively, cells were seeded at equal densities in 12-well plates and after 3 days photographs were taken using Image-Pro Express® at ×10 magnification. To quantitate density, cells were counted in at least three random 1-cm^2 areas. In addition, cells were grown on coverslips and stained with DAPI as described above, and nuclei visualized under epifluorescence microscopy were counted.

Wound Healing Growth Assay—Cells were plated on 24-well tissue culture plates at 2×10^4 cells/ml/well. After cells reached confluence, the cell layer was scratched using a 1–200-μl pipette tip (38). Cell cultures were photographed at time 0 and at 16 h after the appropriate treatment, and *Image-Pro Express*® was used to measure the cell monolayer wound distances. Stock solutions of 1 mM FSK, PMA, and Gö6983 were prepared in DMSO and diluted to appropriate concentrations in tissue culture media immediately before use. The control cells were treated with medium containing 0.1% DMSO.

siRNA—Transfections with anti-*VACM-1* siRNAs targeting different regions of the VACM-1/Cul5 sequence were performed according to the protocol in the *Silencer*® siRNA starter kit purchased from Ambion® (catalog number AM16708A). Three specific antisense oligonucleotides in the *Silencer*® predesigned siRNA included siRNA 1 (5′-AGAUUCCUGGCGUAAAAGCtt-3′) (ID 192207), siRNA 2 (5′-CCACGUAUCAAGCAUGAGCtt-3′) (ID 192208), and siRNA 3 (5′-UAGCAUCAUUAACAACUGCtt-3′) (ID 192209). The control cells were sham-transfected. For the negative control, cells were transfected with siRNAs that did not target any gene sequences provided in the starter kit. The positive control used was GAPDH siRNA provided in the starter kit. In some experiments, double transfection was performed after 24 h, and cell lysates were collected at 48 h (9).

Immunoprecipitation—Total lysates (100–300 μg of protein) prepared from asynchronous cells were resuspended in 150 μl of solubilization buffer (50 mM Tris HCl, pH 8, 150 mM NaCl, 0.3% Triton X-100, 1 mM Pefabloc®SC, and 10 μg/ml aprotinin) and incubated with a 1:250 dilution of affinity-purified Ab-A (directed against the N-terminal sequence of VACM-1 protein), anti-Nedd8 Ab, anti-phospho-PKA substrate (RR*X*(S/T)) Ab (Cellular Signaling Technology) (30), or a nonspecific antibody. After 2 h of incubation, protein A-Sepharose (Amhersham Biosciences) suspension was added, and the incubation continued for another 2 h. The complex was centrifuged at 12,000 rpm for 2 min and washed 2–3 times in the solubilization buffer. Loading dye was added, and the immunoprecipitates were heated to 95 °C for 5 min, separated using 12.5% SDS-polyacrylamide gels, transferred to nitrocellulose, and probed with an antibody directed against VACM-1 protein, as described below (5, 36).

Western Blot Analysis—Total cell lysates and membrane fractions were prepared as described previously (5). Cells were grown to at least 70% confluence, washed in ice-cold PBS, and

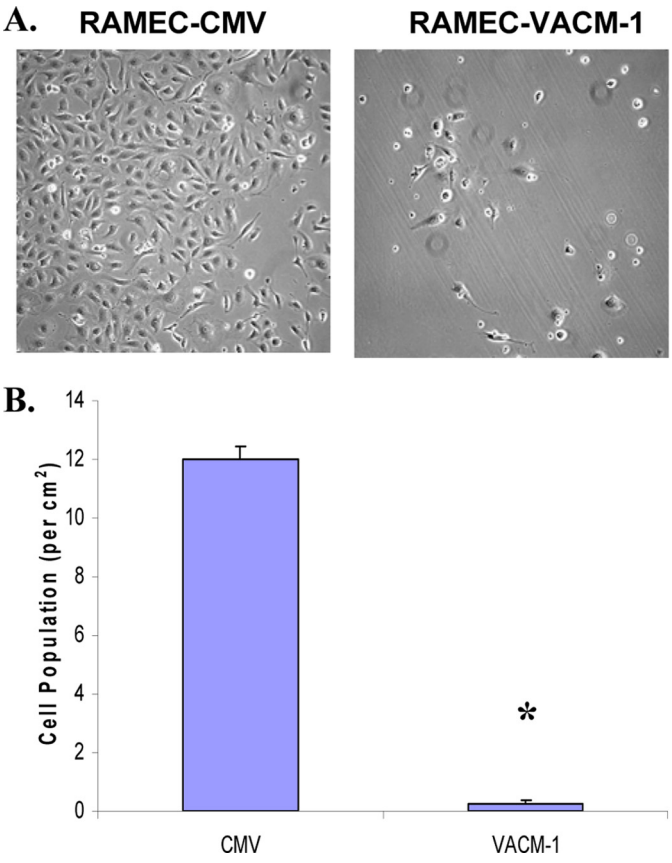

FIGURE 1. **Overexpression of *VACM-1* cDNA in rat endothelial cells; RAMEC inhibits cellular growth.** *A*, representative phase-contrast microscopy results showing decreased cell growth in *VACM-1*-transfected cells when compared with the CMV-transfected cells at 3 days. RAMEC expressing endogenous VACM-1 transfected with CMV vector or *VACM-1* cDNA were seeded at equal density, and growth was monitored and quantitated as described under "Experimental Procedures." *B*, cells shown in *A* were counted in triplicate in six independent culture plates. Values are expressed as mean ± S.E. *, $p < 0.05$.

resuspended in 500 μl of buffer (50 mM Tris (pH 7.4), 0.1% Triton X-100, 150 mM NaCl, 1 M EDTA, 50 mM NaF) with 1 μg/ml apoprotinin, 100 μM Pefabloc^{R}SC, and 10 mM phenylmethylsulfonyl fluoride. All samples were homogenized with a Polytron homogenizer, and protein concentration was determined using the Bradford method (Bio-Rad). Nuclear and membrane fractions were isolated as described previously (35). Both nuclear and membrane pellets were resuspended in the buffer, and their protein concentrations were determined as described using the Bradford assay (34). All samples were resuspended in 4× sample buffer (Invitrogen), heated to 95 °C for 5 min, and subjected to SDS-PAGE using a 12.5% running gel. The separated proteins were transferred to a nitrocellulose membrane (Osmotics Co., Trevose, PA) at 30 mV for 2 h. Nonspecific binding was blocked by incubating membrane temperature with PBS containing 5% nonfat dry milk and 0.2% Tween 20 for 30 min at room temperature. When probing with anti-phospho-PKA phosphorylation-specific Ab, blots were blocked with 5% BSA solution. Membranes were next incubated for 2 h at room temperature in buffer solution containing a 1:200 dilution of affinity-purified polyclonal antibodies directed against the N terminus (Ab-A) of VACM-1 protein (1, 36). In some experiments, blots were stripped and reprobed with anti-

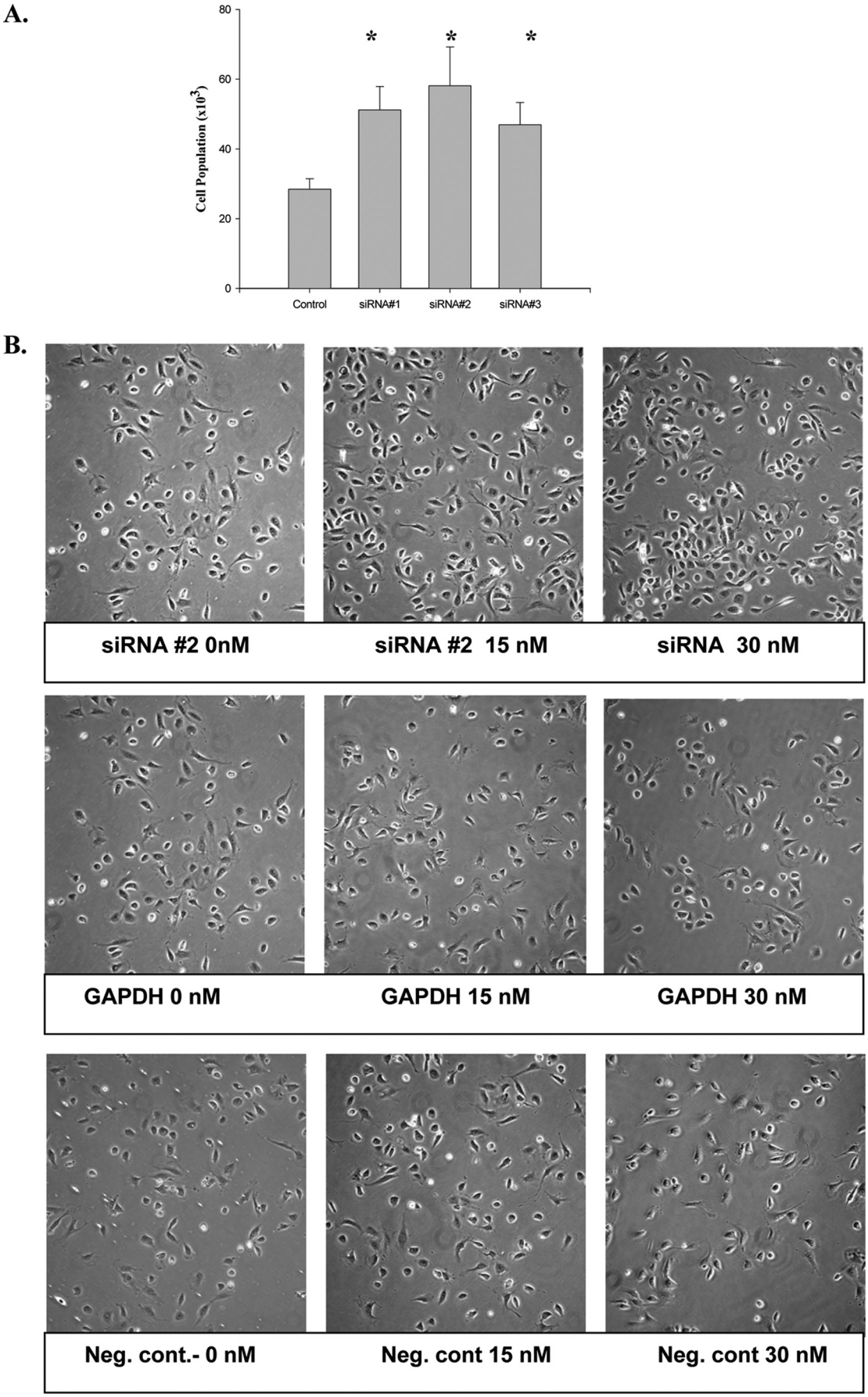
A.
80
60
40
20
0
Cell Population (x10^3)
*
*
*
Control
siRNA#1
siRNA#2
siRNA#3
B.
siRNA #2 0nM
siRNA #2 15 nM
siRNA 30 nM
GAPDH 0 nM
GAPDH 15 nM
GAPDH 30 nM
Neg. cont.- 0 nM
Neg. cont 15 nM
Neg. cont 30 nM

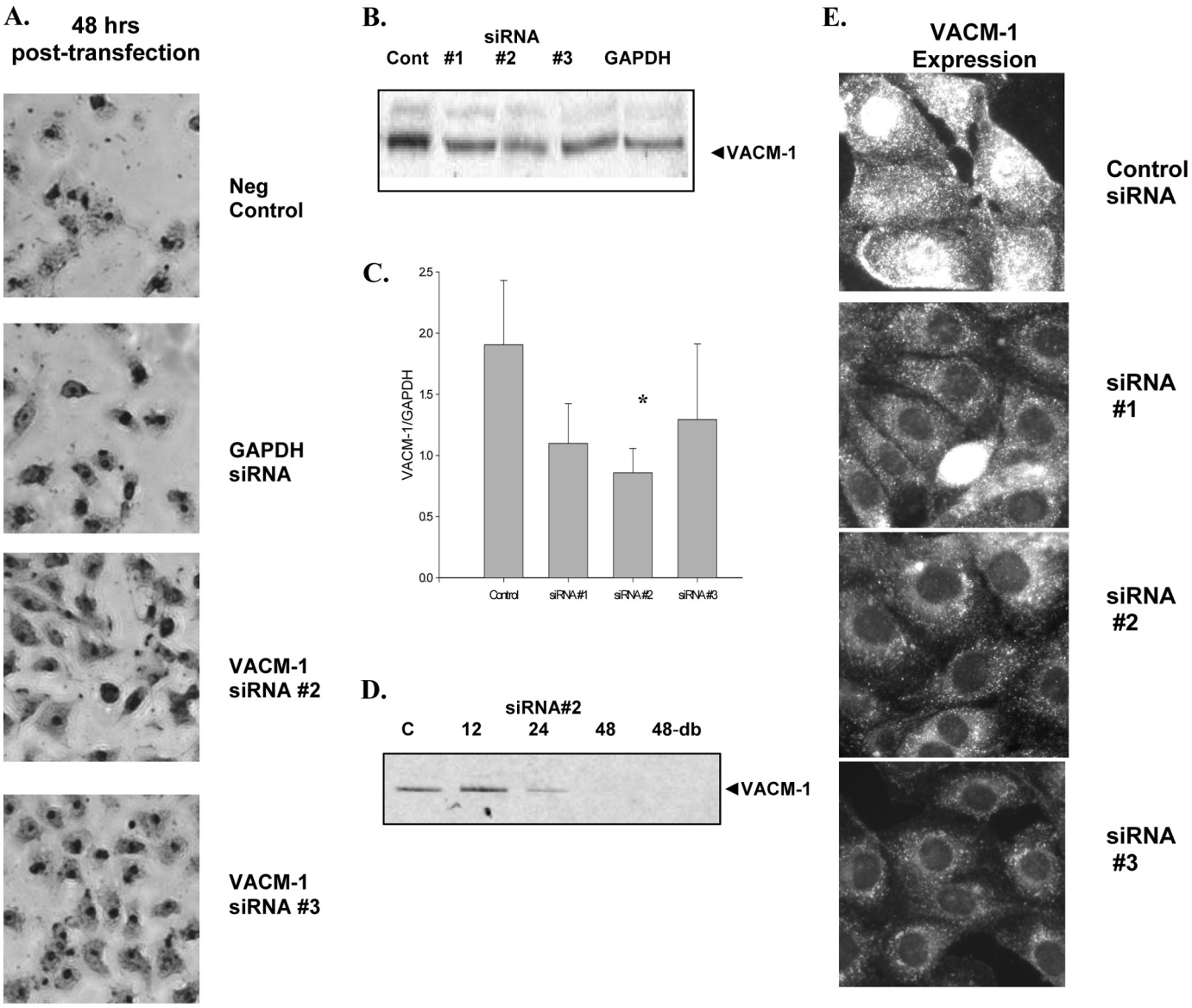

FIGURE 3. ***VACM-1*-specific siRNA oligonucleotides induce cell growth and attenuate VACM-1 protein expression in RAMEC.** *A*, RAMEC seeded at equal density were transfected with a random siRNA (*first panel*), siRNA targeting GAPDH (*second panel*), and siRNAs targeting VACM-1 (#*2* and #*3*, *third* and *fourth panels*) and stained with methylene blue at 48 h after transfection. *B*, Western blot analysis of RAMEC transfected with anti-*VACM-1*-specific siRNA oligonucleotides 1, 2, and 3 and anti-GAPDH siRNA. Lysates were collected at 48 h, quantitated for protein concentration, and resolved by SDS-PAGE. After transfer to the nitrocellulose membrane, blots were probed with anti-VACM-1-specific antibody as described under "Experimental Procedures." To ascertain equal protein loading, membranes were stripped and reprobed with anti-GAPDH Ab (not shown). *C*, the intensity of the signal shown in *B* was quantitated using Image J®, as described under "Experimental Procedures" ($n = 4$; *, $p < 0.05$). *D*, time-dependent effect of 15 nM siRNA 2 on VACM-1 protein expression at 12, 24, and 48 h. In addition, VACM-1 protein concentration was examined in cells double transfected with the 15 nM siRNA 2 at 24 h and collected at 48 h (*48-db*). *E*, a representative immunocytochemistry result demonstrating the effect of 15 nM siRNAs on VACM-1 protein expression at 48 h after transfection. Magnification is ×40 ($n = 3$).

Nedd8-specific Ab (1:500 dilution) developed in rabbits (Alexis Co.). To ascertain equal protein loading, blots were stripped and incubated in a 1:10,000 dilution of monoclonal anti-mouse GAPDH (Abcam Inc.) for 1.5 h at room temperature. The membranes were next washed in the same buffer for 15 min and twice for 5 min and incubated for 2 h with a horseradish peroxidase-conjugated secondary antibodies (diluted at 1:2000 to 1:10,000) (Cell Signaling, Beverly, MA). The nitrocellulose membranes were washed as described above, exposed to the luminol detection reagents (Cell Signaling) for 1 min or longer, if appropriate, and exposed to x-ray film (Amhersham).

Statistical Analysis—Data are expressed as mean ± S.E. SYSTAT® *t* tests were used for data analysis. Significance was set at $p < 0.05$ unless noted otherwise.

FIGURE 2. **Down-regulation of *VACM-1/cul5* with anti-VACM-1-specific siRNA oligonucleotides induces cellular proliferation in RAMEC.** *A*, growth rates in RAMEC, expressing endogenous VACM-1/Cul5 protein and transfected with three siRNA oligonucleotides targeting *VACM-1/cul5* mRNA. All three anti-*VACM-1* siRNA oligonucleotides significantly increased cell growth when compared with the control RAMEC at 24 h. $n = 3$; *, $p < 0.05$. *B*, representative phase-contrast microscopy results showing increased cell growth in RAMEC expressing endogenous VACM-1 protein and transfected with 0, 15, and 30 nM siRNA 2 (*top*). Anti-GAPDH siRNA (*middle*) or a scrambled siRNA (*bottom*) was used as a control. *Neg. cont.*, negative control.

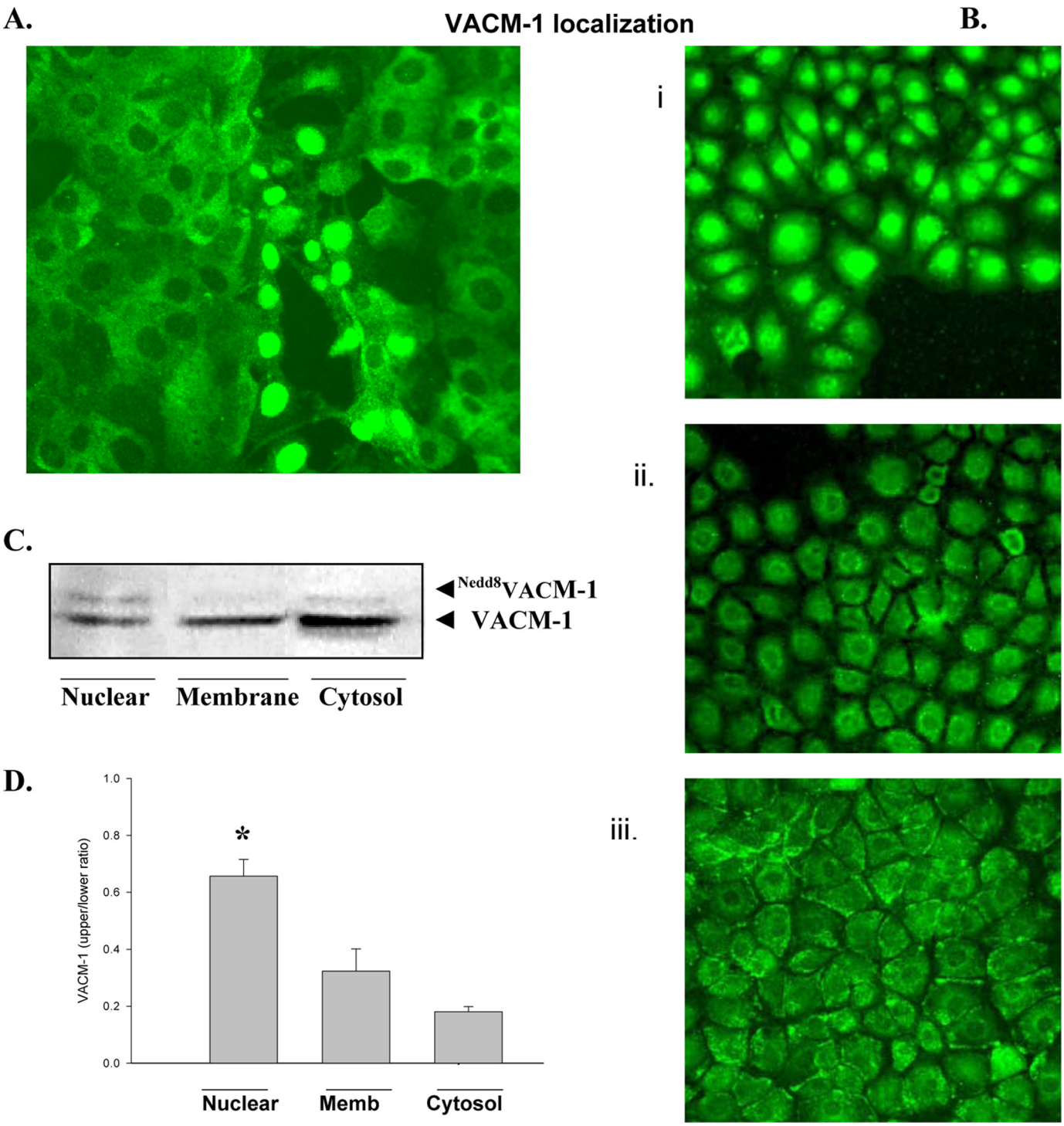

FIGURE 4. **Cellular localization of endogenous VACM-1 protein in RAMEC is dependent on cell cycle.** *A* and *B*, RAMEC grown to confluence on glass coverslips were "wounded" with a pipette tip and allowed to grow into the "wound." Cellular growth was monitored microscopically. Cells were fixed and immunostained with anti-VACM-1-specific antibody as described under "Experimental Procedures." *B*, a representative immunostaining of different regions from the same coverslip shown in *A*; the immunostaining was in the wound (*i*), close to the wound (*ii*), and distant from the wound (*iii*). *C*, Western blot analysis of nuclear, membrane, and cytosolic cell fractions collected from asynchronous RAMEC grown for 48 h and resolved by SDS-PAGE, transferred to nitrocellulose, and probed with anti-VACM-1 Ab. *D*, signal intensity for VACM-1/Cul5 protein and modified VACM-1/Cul5 were quantitated and presented as a ratio of the upper to the lower band ($n = 3$; *, $p < 0.05$).

RESULTS

To confirm the antiproliferative effects of VACM-1/Cul5 *in vitro*, RAMEC expressing endogenous VACM-1 protein (36) were transfected with *VACM-1* cDNA. The growth of these cells was monitored as described under "Experimental Procedures" (9). The CMV vector-transfected RAMEC were confluent 3 days after plating compared with the minimal growth of the *VACM-1* cDNA-transfected cells (Fig. 1*A*). When cell growth was quantitated, there was a significant difference in growth rates between the two groups. The *VACM-1*

cDNA-transfected RAMEC failed to reach confluence 1 week after plating (data not shown).

To further ascertain the antiproliferative effect of VACM-1, we transfected cells with three anti-*VACM-1*/*cul5*-specific siRNA oligonucleotides (Ambion Inc.). Time-dependent (24 and 48 h) and dose-dependent (0 nM control, 15 nM, and 30 nM) effects of the anti-*VACM-1*/*cul5*-specific oligonucleotides were examined using light microscopy and Western blot analysis. Our results (Fig. 2) demonstrate that RAMEC transfected with any of the three anti-*VACM-1*-specific siRNA oligonucleotides for 24 h grew significantly faster than the control cells (Fig. 2*A*, $n = 3$ each; *, $p < 0.05$). A representative photograph for cells treated with siRNA 2 is shown in Fig. 2*B* (*top*). There was no significant difference in RAMEC growth rate between control cells and those cells transfected with the GAPDH siRNA, which was used as a positive siRNA control (Fig. 2*B*, *middle*). The negative control siRNA, which did not target any particular sequence, was used to evaluate the transfection efficiency, and it had no effect on cell growth (Fig. 2*B*, *bottom*). The growth-promoting effects of anti-VACM-1-specific siRNA oligonucleotides were further confirmed at 48 h after transfection using a methylene blue staining technique (Fig. 3*A*).

To establish that the increase in cell growth was associated with changes in VACM-1 protein concentration, cell lysates from control and anti-VACM-1-specific siRNA oligonucleotide-transfected cells were examined for VACM-1 protein expression using the Western blot approach. VACM-1/Cul5 signal was quantified and corrected for GAPDH protein concentration. Our results (Fig. 3, *B* and *C*) show a decrease in VACM-1 protein concentration in RAMEC treated with all oligonucleotides at 24 h posttransfection, but the decrease was statistically significant only in the group treated with siRNA 2 ($n = 4$, $p < 0.05$). The decrease in VACM-1/Cul5 protein expression after treatment with siRNA oligonucleotides was time-dependent. A representative blot for lysates prepared from cells transfected with siRNA 2 and collected at different time points is shown in Fig. 3*D*. The highest decrease in VACM-1/Cul5 protein concentration was observed in RAMEC retransfected with the siRNA at 24 h and harvested at 48 h (*48-db* in Fig. 3). To further confirm the effectiveness of the siRNA constructs, we performed immunocytochemistry experiments. The data shown in Fig. 3*E* further support Western blot analysis results. In cells transfected with all three anti-*VACM-1*/*cul5* siRNAs and stained with anti-VACM-1/Cul5-specific Ab at 24 h after transfection, a clear decrease in the signal was observed with all oligonucleotides tested when compared with the control group. Together, these findings establish the inhibitory effect of VACM-1 on cellular proliferation previously described (5, 6, 9).

Previous work suggested that endogenous VACM-1 is localized to the cell membrane or cytosol when cells are not dividing, and VACM-1 is nuclear when cells are dividing (9, 36). To further examine the subcellular localization of VACM-1 protein in RAMEC at different stages of the cell cycle, we used a wound healing assay. In this technique, proliferating and nonproliferating cells from the same culture are represented on the same slide. Immunocytochemistry data using anti-VACM-1 Ab suggest that in the proliferating cells, VACM-1 protein was local-

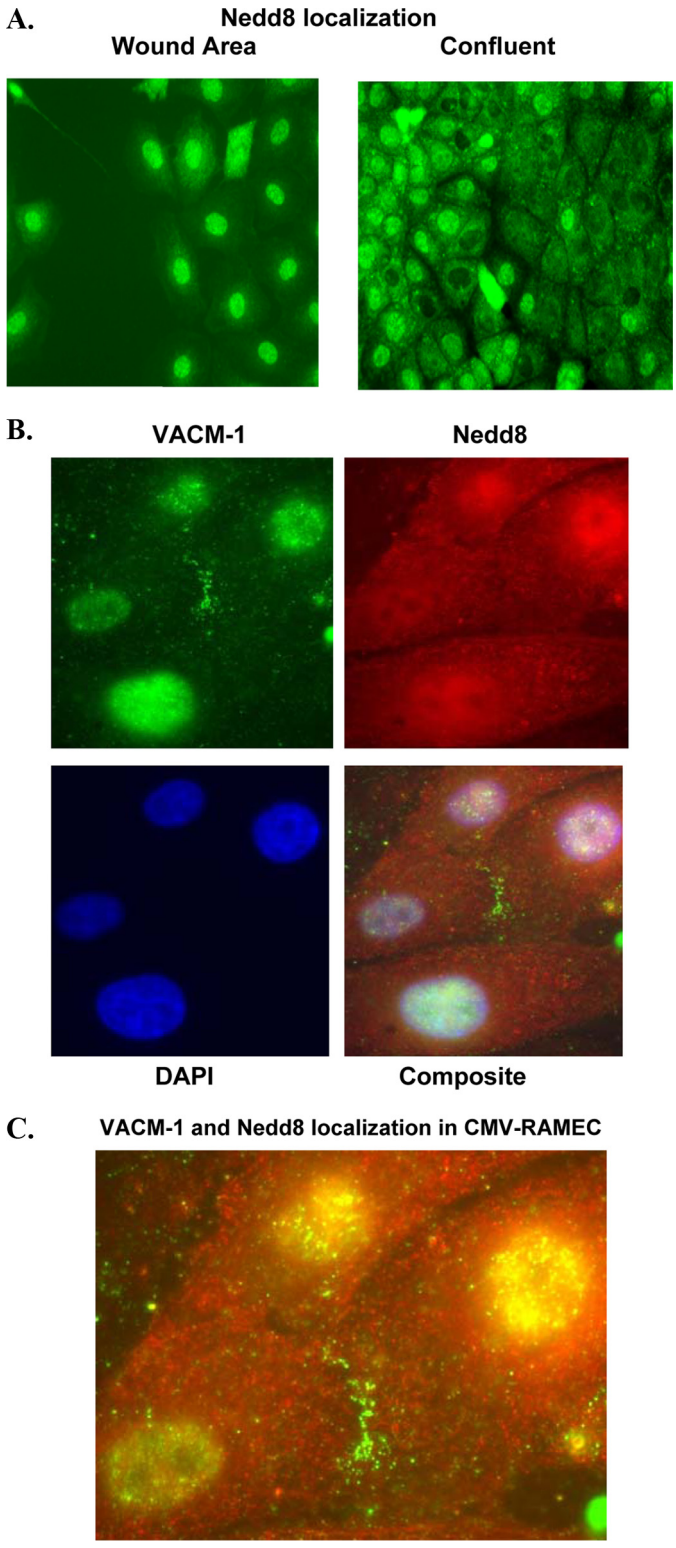

FIGURE 5. **Nedd8-specific modification of VACM-1/Cul5 protein is localized to the nucleus.** *A*, RAMEC grown to confluence on glass coverslips were wounded with a pipette tip and allowed to grow into the wound. Immunostaining experiments described in the legend to Fig. 4*A* were repeated using anti-Nedd8-specific Ab. The immunostaining in the wound and in a confluent region distant from the wound is shown. Magnification is ×40. *B*, cells were fixed and immunostained with anti-VACM-1-specific Ab (*green*), anti-Nedd8-specific antibody (*red*), and DAPI (*blue*) as described under "Experimental Procedures." Nuclear staining was performed using DAPI (magnification, ×100). *C*, overlay of VACM-1/Cul5 and Nedd8 protein localization in the nuclear but not the membrane region in control RAMEC.

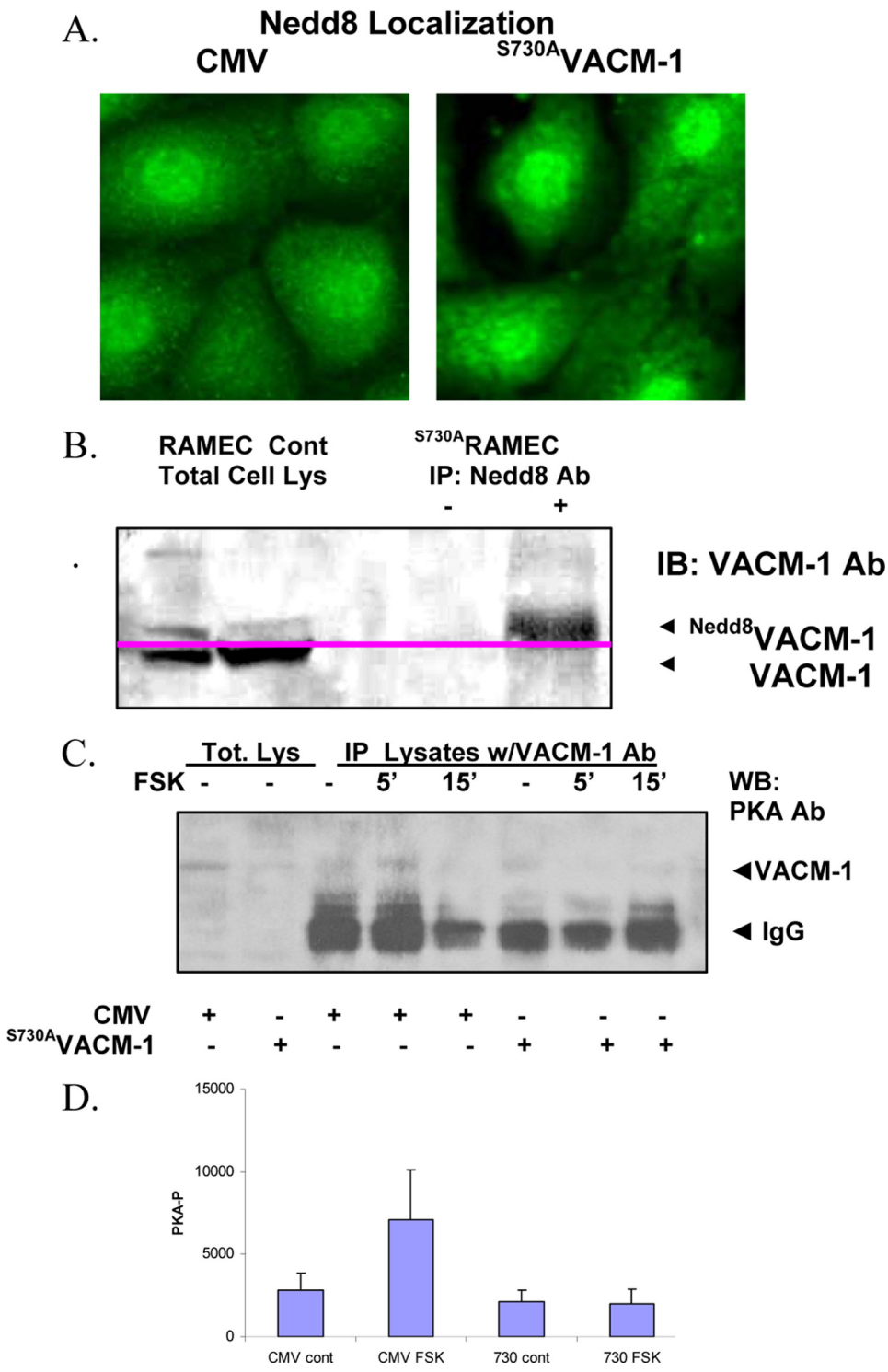

FIGURE 6. **Nedd8- specific modification of VACM-1/Cul5 protein is regulated by PKA activity.** *A*, immunostaining of CMV and ^{S730A}*VACM-1* cDNA-transfected RAMEC with anti-Nedd8 antibodies showed increased Nedd8 signal in ^{S730A}*VACM-1* cDNA-transfected RAMEC when compared with controls. *B*, removal of the PKA phosphorylation site in VACM-1/Cul5 protein (S730A) sequence increases modification of VACM-1 by Nedd8. Lysates from ^{S730A}*VACM-1*-transfected cells were immunoprecipitated with the polyclonal anti-Nedd8 antibodies and probed with anti-VACM-1 Ab as described under "Experimental Procedures." Total cell lysates from CMV-transfected RAMEC were used as a control. *C*, PKA-dependent phosphorylation of VACM-1/Cul5 is attenuated in ^{S730A}*VACM-1* cDNA-transfected cells when compared with controls. CMV and ^{S730A}VACM-1 cDNA-transfected RAMEC were treated with 10 μM FSK for 5 or 15 min. Total cell lysates (100 μg) were immunoprecipitated with anti-VACM-1-specific antibody and protein A/Sepharose as described under "Experimental Procedures." The immunoprecipitates were resolved by SDS-PAGE. After transfer to the nitrocellulose membrane, blots were probed with anti-phospho-PKA substrate-specific Ab, as described under "Experimental Procedures." Lysate from CMV-transfected RAMEC were used as a control. *D*, signal intensity shown in *C* was quantitated and compared ($n = 3$; *, $p < 0.2$). *IP*, immunoprecipitation; *IB*, immunoblot.

ized to the nucleus (Fig. 4, *A* and *B* (*i*)), whereas in the nonproliferating cells VACM-1/Cul5 was cytosolic (Fig. 4, *A* and *B* (*ii*)) or cell membrane-specific (Fig. 4, *A* and *B* (*iii*)). Interestingly, when lysates from asynchronous RAMEC were separated into the nuclear, cytosolic, and membrane fractions and separated by SDS-PAGE for immunoblotting with anti-VACM-1 Ab (35), the nuclear but not the cytosolic or the membrane fractions demonstrated the presence of a larger M_r species that could be recognized by anti-VACM-1 Ab (Fig. 4*C*). When the signal was quantitated and expressed as a ratio of the upper to the lower band, there was a significant difference between the nuclear and membrane or cytosolic fractions (Fig. 4*D*, $n = 3$; *, $p < 0.05$).

The appearance of a larger M_r species on Western blot was previously identified as Nedd8-modified VACM-1 protein (5, 9). Consequently, the wound healing assay described above was used to examine the Nedd8 signal in proliferating and nonproliferating cells. Our results indicate that in the wound area where cells are proliferating, the Nedd8 signal is very intense and localizes to the nucleus, whereas in the nonproliferating regions of the cell culture, the Nedd8 signal is reduced or absent (Fig. 5*A*). The coimmunostaining experiments using anti-VACM-1/Cul5-specific Ab (*green*) and anti-Nedd8-specific Ab (*red*) indicate that VACM-1 and Nedd8 signal colocalize in the nuclear region but not in the cell membrane (Fig. 5, *B* and *C*).

To investigate this effect further, we next used a cell line expressing the ^{S730A}*VACM-1* cDNA mutant (5, 9). We have shown previously that in cells transfected with ^{S730A}*VACM-1* cDNA, where the PKA-specific phosphorylation site has been mutated (5, 9), VACM-1 protein is highly neddylated and localizes to the nucleus. Our immunostaining results shown in Fig. 6*A* confirm that the Nedd8-specific signal was increased in the ^{S730A}*VACM-1* cDNA-transfected

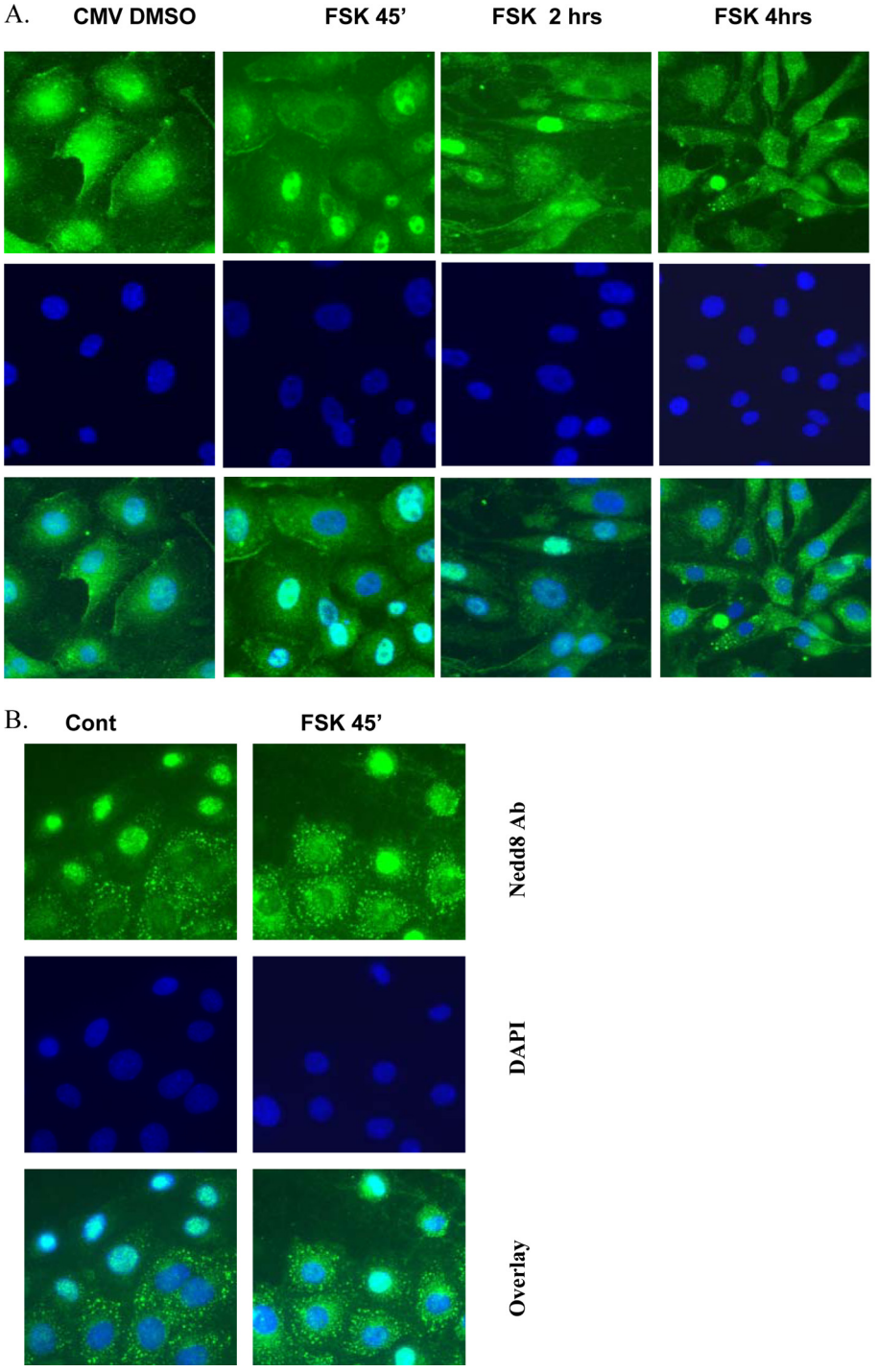

FIGURE 7. **Nuclear localization of VACM-1 and Nedd-8 is regulated by PKA.** *A*, control cells treated with 10 μM FSK for at least 45 min (*FSK 45'*), 2 h, and 4 h were fixed and immunostained with anti-VACM-1-specific antibody as described under "Experimental Procedures." Nuclear staining was monitored with DAPI. To show the disappearance of nuclear localization of VACM-1 protein after treatment with FSK, the three signals were overlaid. The edge of the wound area is at the *top* of the slide. *B*, cells treated with 10 μM FSK for at least 45 min were fixed and immunostained with polyclonal anti-Nedd8-specific antibody as described under "Experimental Procedures." Nuclear staining was monitored with DAPI. To show the disappearance of nuclear localization of VACM-1 protein after treatment with FSK, the signals were overlaid. The edge of the wound area is at the *top* of the slide. *Cont*, control.

RAMEC when compared with the control cells. Further, the immunoprecipitation study, where anti-Nedd8 Ab was used to "pull-down" proteins and anti-VACM-1 Ab was used to probe the blot, showed that only the higher M_r species was detected (Fig. 6*B*). These results suggested, therefore, that neddylation of VACM-1 protein may be regulated by PKA-dependent phosphorylation at Ser-730.

Thus, we next explored the hypothesis that the rapid translocation of VACM-1 protein from the nuclear region in nonconfluent cells to the cytosol and/or membrane in the confluent cells (Fig. 4) depends on modification of VACM-1 by Nedd8 and is regulated by PKA. To induce PKA activity, CMV- and ^{S730A}*VACM-1* cDNA-transfected cells were treated with 10 μM forskolin for 5 or 15 min as described (30, 37). Total cell lysates were collected and immunoprecipitated with anti-VACM-1-specific Ab. Samples were resolved on SDS-PAGE, and after transfer to nitrocellulose, blots were probed with an antibody that recognizes PKA-phosphorylated proteins (30, 37). Our results show that PKA-dependent phosphorylation of VACM-1/Cul5 is higher in the CMV-transfected cells when compared with the ^{S730A}*VACM-1* cDNA-transfected cells (Fig. 6*C*, *first two lanes*). PKA-specific signal was increased in all experiments from control cells treated with FSK for 5 min (3787 ± 849 *versus* 7559 ± 2915, $n = 4$, $p < 0.2$). No change in signal intensity was observed in ^{S730A}*VACM-1* cDNA-transfected cells (2111 ± 703 *versus* 2024 ± 844, $n = 3$, not significant). Interestingly, only the 91-kDa VACM-1/Cul5 and not the higher M_r species identified in Fig. 6*B* as the neddylated VACM-1/Cul5 was immunoprecipitated with the anti-phospho-PKA substrate-specific antibody (Fig. 6, *C* and *D*). To extend these experiments even further, we used the immunocytochemistry approach. The representative data shown in Fig. 7*A* indicate that treatment of control cells with FSK (10 μM) to increase PKA activity reduced nuclear localization of VACM-1/Cul5 protein. This effect was rapid because VACM-1/Cul5 signal intensity was decreased in 45 min and totally disappeared at 2 and 4 h after treatment. Similarly, we observed that in the proliferating cells (wound area) treated with forskolin for 45

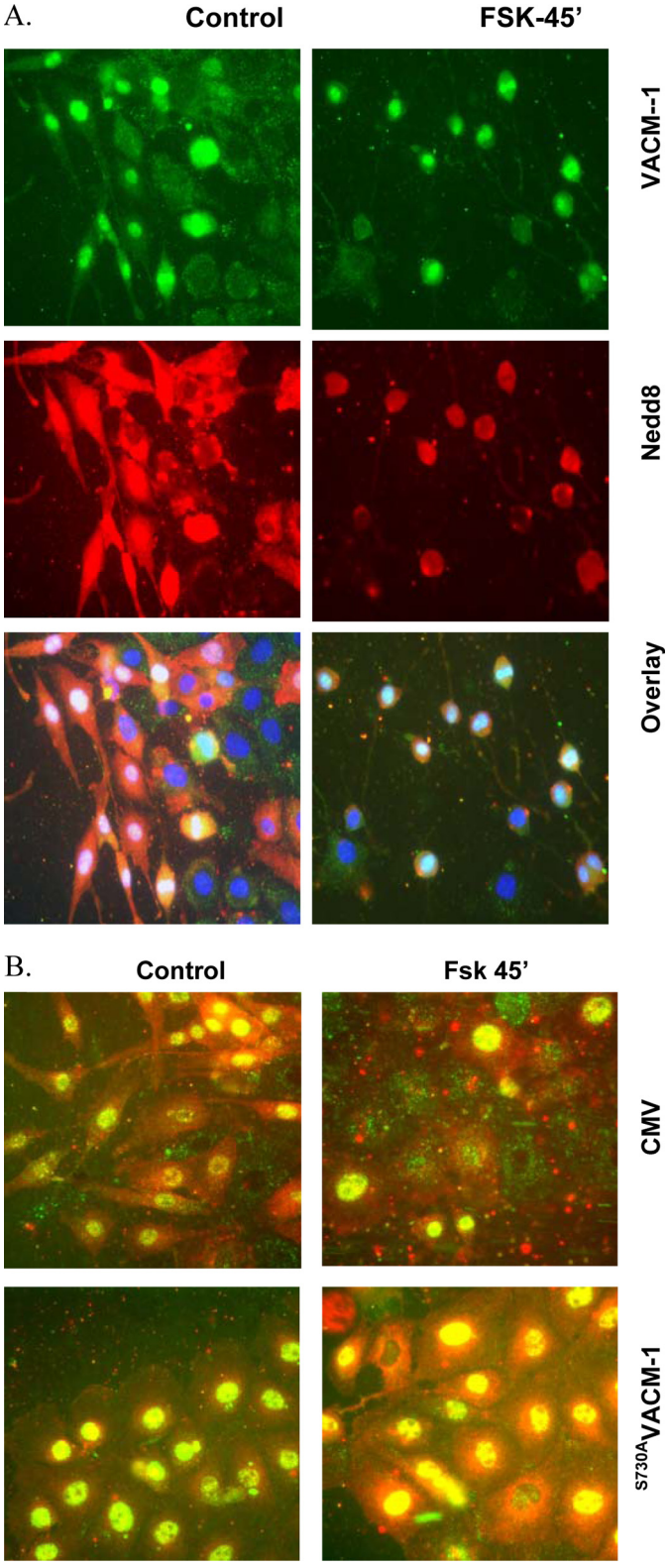

FIGURE 8. **Forskolin-induced activation of PKA reduces nuclear localization of VACM-1 and Nedd8 in control but not ^{S730A}*VACM-1* cDNA-transfected cells.** *A*, control cells treated with 10 μM FSK for at least 45 min (*FSK-45'*) were fixed and immunostained with anti-VACM-1-specific (*green*) and anti-Nedd8-specific (*red*) antibodies, as described under "Experimental Procedures." Nuclear staining was monitored with DAPI. To show the disappearance of nuclear localization of VACM-1 protein after treatment with FSK, the signals were overlaid. The edge of the wound area is at the *top left* of the slide. *B*, control and ^{S730A}*VACM-1* cDNA-transfected cells treated with 10 μM FSK for at least 45 min were fixed and immunostained as described above (*A*). To show the disappearance of nuclear localization of VACM-1 protein after treatment with FSK, the signals were overlaid. The edge of the wound area is at the *top left* of the slide.

min and stained with anti-Nedd8-specific Ab, Nedd8 signal was reduced as well (Fig. 7*B*).

To ascertain the specificity of this effect, these experiments were repeated using a double immunostaining approach. Our results shown in Fig. 8*A* indicated that in control cells, Nedd8 and VACM-1/Cul5 signals in the proliferating cells are largely overlapping. Induction of PKA activity with FSK resulted in a decreased signal intensity. Interestingly, in cells expressing the mutated *VACM-1* cDNA lacking the PKA phosphorylation site, treatment with Fsk for 45 min did not appear to affect localization of either protein (Fig. 8*B*, *bottom*).

In addition to the PKA-specific phosphorylation site at Ser-730 and the neddylation site at Lys-724, 15 putative PKC-specific phosphorylation sites can be identified in VACM-1 sequence (5). To further examine VACM-1 phosphorylation status in ^{S730A}*VACM-1* cDNA-transfected RAMEC, we examined whether VACM-1 signal intensity was affected by treatment of cell lysates with either 300 μM okadaic acid to inhibit endogenous phosphatases or by treatment with 100 units/ml calf intestinal phosphatase to decrease protein phosphorylation (38). Lysate samples pretreated with calf intestinal phosphatase had lower signal intensity compared with the control or with the okadaic acid-treated lysates (Fig. 9*A*), suggesting that in the absence of the PKA phosphorylation site, VACM-1 may still be phosphorylated.

To examine whether PKC plays a role in the regulation of VACM-1-dependent cell growth, cells were treated with PMA to induce PKC activity and with Gö6983 to inhibit its activity (37). The time-dependent and dose-dependant effect of PMA and Gö6983 were established (data not shown). Representative light microscopy results of the wound healing assay for the CMV control and ^{S730A}*VACM-1* cDNA-transfected cells treated with 10 and 100 nM PMA and 7 nM Gö6983 are shown in Fig. 9*B*. When data shown in Fig. 9*B* were quantitated, we observed a significant increase in cell growth in both groups treated with PMA. However, the increase in ^{S730A}*VACM-1* cDNA-transfected RAMEC was significantly higher when compared with the control group ($n = 5$; *, $p < 0.05$). Further, when PKC activity was inhibited with 10 nM Gö6983, cell growth was decreased in ^{S730A}*VACM-1* cDNA-transfected cells significantly more than in the control group ($n = 5$; *, $p < 0.05$).

DISCUSSION

In this study, we report several new findings that enhance our understanding of the mechanism by which VACM-1/Cul5 protein regulates cellular growth. First, we confirmed that overexpression of *VACM-1*/*cul5* cDNA in the rat endothelial cell line inhibits cellular growth, whereas treatment of RAMEC with siRNA oligonucleotides targeting endogenous *VACM-1*/*cul5* leads to an increased cell growth (Figs. 1–3). Second, we demonstrated that the subcellular localization of VACM-1/Cul5 protein may be controlled by its posttranslational modifications (Fig. 4). Further, we showed that the nuclear but not cytosol or membrane-localized VACM-1/

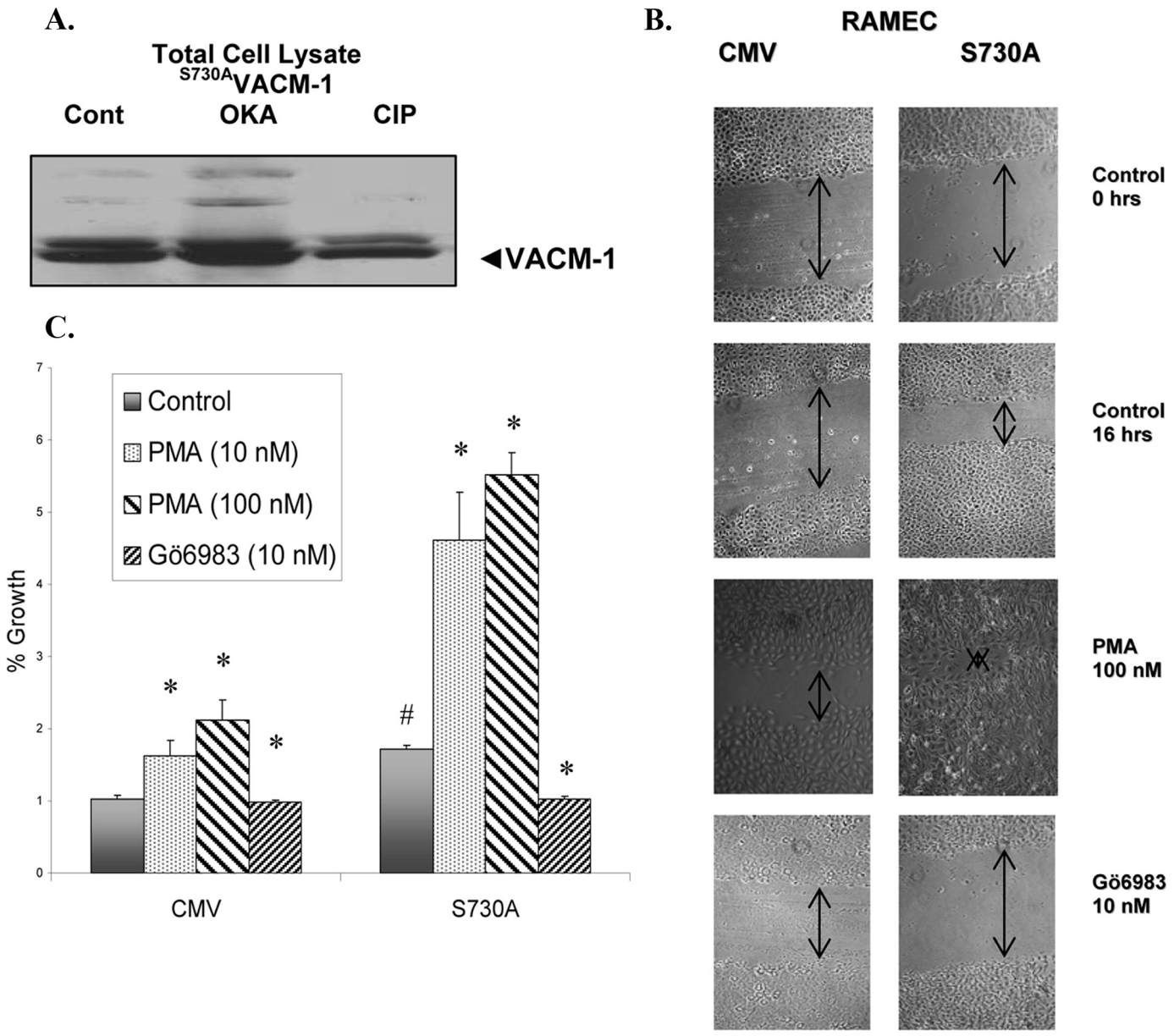

FIGURE 9. **Regulation of VACM-1/Cul5-dependent cell growth by PKC.** *A*, total lysates from ^{S730A}*VACM-1* cDNA-transfected RAMEC were divided equally and incubated with either okadaic acid (*OKA*; 300 μM) or calf intestinal phosphatase (*CIP*; 100 units/ml) for 30 min. Lysates were resolved by SDS-PAGE, and after transfer to the nitrocellulose membrane, blots were probed with anti-VACM-1-specific antibody as described under "Experimental Procedures." *B*, wound healing assay from CMV-transfected control and ^{S730A}*VACM-1* cDNA-transfected RAMEC. Confluent cell cultures were wounded with a pipette tip, and cell regrowth was observed under an inverted phase-contrast microscope (Nikon). Photographs were taken at time 0 and 16 h after treatment with the vehicle, PMA (10 and 100 nM), and Gö6983 (7 nM), as described under "Experimental Procedures." *C*, the effects of PMA and Gö6983 shown in *A* were quantitated ($n = 5$; *, $p < 0.001$).

Cul5 protein is modified by Nedd8 protein (Fig. 5). Third, we showed that neddylation of VACM-1/Cul5 protein is controlled by PKA-specific phosphorylation at Ser-730 (Figs. 6–8). Finally, we found that stimulation of PKC activity with PMA induced cell proliferation significantly higher in cells transfected with ^{S730A}*VACM-1* cDNA when compared with the control, where the PKA-specific phosphorylation site was intact (Fig. 9). Our results suggest for the first time that neddylation of VACM-1/Cul5, itself controlled by the PKA-dependent phosphorylation, may regulate its subsequent phosphorylation by PKC.

Phosphorylation is a rapid and effective way to change cellular localization and the function of a protein (39). Both PKA- and PKC-specific phosphorylation regulate cellular function of many proteins in health and disease (30–33, 40). For example, PKA regulates nucleo-cytoplasmic shuttling of a transcription factor Id1 during angiogenesis (32) and is identified as an inhibitory component in the Gli protein translocation to the nucleus (33). Activation of PKA leads to the retention of Gli in the cytoplasm, whereas inhibition of PKA activity promotes its nuclear localization. Similarly, PKC-dependent phosphorylation of specific proteins and its role in cellular processes like angiogenesis, a crucial step in tumor development, has been established (41). Further, the transition from the phosphorylated to the nonphosphorylated form of the Fas-associated death domain-containing protein, associated

with carcinogenesis (42), has been used as a marker for cancer progression (43). Although the phosphorylation of the proteasome's subunits by specific kinases has been reported (12, 16), our results are the first to show that posttranslational modifications of VACM-1/Cul5 protein by Nedd8 is controlled by PKA-specific phosphorylation.

VACM-1/cul5 is the least conserved member of the cullin family, and its biological significance is only emerging. To date, Cul5-dependent E3 ubiquitin ligase complexes have been shown to control the adenovirus-induced p53 degradation *in vitro* and the degradation of proteins essential for the prevention of HIV infectivity (44, 45). I*n vivo*, expression of VACM-1/Cul5 protein is largely endothelium-specific (8, 9). When expressed in several cell lines *in vitro*, VACM-1/Cul5 inhibits MAPK phosphorylation and nuclear localization of Egr-1, signaling molecules recognized for their role in the regulation of cellular proliferation (5, 9). These effects appear to be dependent on the state of VACM-1 modification by Nedd8 because in cells transfected with the ^{S730A}*VACM-1* cDNA, phosphorylation of MAPK was directly correlated to the level of neddylated VACM-1 protein (5). Interestingly, Nedd8 conjugation to cullins is believed to be fundamental for the activity and stability of numerous E3 ligases (46). Further, it has been reported that cullins must be neddylated and form heterodimers to be an active component of the E3 ligase complex (14). This proposed model supports the dominant negative phenotype observed in ^{S730A}*VACM-1* cDNA-transfected endothelial cells *in vitro* (5). Importantly, a recent report targeting the Nedd8-specific pathway for development of anti-cancer drugs (47) further underscores the significance of our findings.

In summary, this study shows that PKA-dependent phosphorylation of VACM-1/Cul5 regulates its neddylation and subsequent phosphorylation by PKC. Because the neddylation process is now a target for development of new drugs to regulate excessive cellular proliferation (47), understanding the underlying mechanism at the cellular level is critical.

REFERENCES

1. Burnatowska-Hledin, M., Spielman, W. S., Smith, W. L., Shi, P., Meyer, J. M., and Dewitt, D. L. (1995) *Am. J. Physiol.* (*Renol.*) **268,** F1198–F1210
2. Byrd, P. J., Stankovic, T., McConville, C. M., Smith, A. D., Cooper, P. R., and Taylor, A. M. (1997) *Genome Res.* **7,** 71–75
3. Kipreos, E. T., Lander, L. E., Wing, J. P., He, W. W., Hedgecock, E. M. (1996) *Cell* **85,** 829–839
4. Mathias, N., Johnson, S. L., Winey, M., Adams, A. E., Goetsch, L., Pringle, J. R., Byers, B., and Goebl, M. G. (1996) *Mol. Cell. Biol.* **16,** 6634–6643
5. Van Dort, C., Zhao, P., Parmelee, K., Capps, B., Poel, A., Listenberger, L., Card, B., Murrey, D., Kossoris, J., and Burnatowska-Hledin, M. (2003) *Am. J. Physiol.* (*Cell*) **285,** C1386–C1396
6. Johnson, A. E., Le, I. P., Buchwalter, A., and Burnatowska-Hledin, M. A. (2007) *Mol. Cell. Biochem.* **301,** 13–20
7. Burnatowska-Hledin, M. A., Kossoris, J. B., Van Dort, C. J., Shearer, R. L., Zhao, P., Murrey, D. A., Abbott, J. L., Kan, C. E., and Barney, C. C. (2004) *Biochem. Biophys. Res. Commun.* **319,** 817–825
8. Burnatowska-Hledin, M., Lazdins, I. B., Listenberger, L., Zhao, P., Sharangpani, A., Folta, V., and Card, B. (1999) *Am. J. Physiol.* (*Renol.*) **276,** F199–F209
9. Buchwalter, A., Van Dort, C., Schultz, S., Smith, R., Le, I. P., Abbott, J. L., Oosterhouse, E., Johnson, A. E., Hansen-Smith, F., and Burnatowska-Hledin, M. (2008) *Microvasc. Res.* **75,** 155–168
10. Denti, S., Fernandez-Sanchez, M. E., Rogge, L., and Bianchi, E. (2006) *J. Biol. Chem.* **281,** 32188–32196
11. Saha, A., and Deshaies, R. J. (2008) *Mol. Cell.* **32,** 21–31
12. Petroski, M. D., and Deshaies, R. J. (2005) *Nat. Rev. Mol. Cell Biol.* **6,** 9–20
13. Sun, Y. (2003) *Cancer Biol. Ther.* **2,** 623–629
14. Chew, E. H., Poobalasingam, T., Hawkey, C. J., and Hagen, T. (2007) *Cell. Signal.* **19,** 1071–1080
15. Kamura, T., Koepp, D. M., Conrad, M. N., Skowyra, D., Moreland, R. J., Iliopoulos, O., Lane, W. S., Kaelin, W. G., Jr., Elledge, S. J., Conaway, R. C., Harper, J. W., and Conaway, J. W. (1999) *Science* **284,** 657–661
16. Herrmann, J., Ciechanover, A., Lerman, L. O., and Lerman, A. (2004) *Cardiovasc. Res.* **6,** 11–21
17. Gallagher, E., Gao, M., Liu, Y. C., and Karin, M. (2006) *Proc. Natl. Acad. Sci. U.S.A.* **103,** 1717–1722
18. Gao, M., Labuda, T., and Xia, Y. (2004) *Science* **306,** 271–275
19. Dornan, D., Shimizu, H., Mah, A., Dudhela, T., Eby, M., O'rourke, K., Seshagiri, S., and Dixit, V. M. (2006) *Science* **313,** 1122–1126
20. Hori, T., Osaka, F., Chiba, T., Miyamoto, C., Okabayashi, K., Shimbara, N., Kato, S., and Tanaka, K. (1999) *Oncogene* **18,** 6829–6834
21. Kamitani, T., Kito, K., Nguyen, H. P., and Yeh, E. T. (1997) *J. Biol. Chem.* **272,** 28557–28562
22. Wada, H., Yeh, E. T., and Kamitani, T. (1999) *Biochem. Biophys. Res. Commun.* **257,** 100–105
23. Pan, Z. Q., Kentsis, A., Dias, D. C., Yamoah, K., and Wu, K. (2004) *Oncogene* **23,** 1985–1997
24. Norman, J. A., and Shiekhattar, R. (2006) *Biochemistry* **45,** 3014–3019
25. Liakopoulos, D., Büsgen, T., Brychzy, A., Jentsch, S., and Pause, A. (1999) *Proc. Natl. Acad. Sci. U.S.A.* **96,** 5510–5515
26. Mohanty, S., Lee, S., Yadava, N., Dealy, M. J., Johnson, R. S., and Firtel, R. A. (2001) *Genes Dev.* **15,** 1435–1448
27. Tateishi, K., Omata, M., Tanaka, K., and Chiba, T. (2001) *J. Cell Biol.* **155,** 571–579
28. Kurz, T., Pintard, L., Willis, J. H., Hamill, D. R., Gönczy, P., Peter, M., and Bowerman, B. (2002) *Science* **295,** 1294–1298
29. Salinas, G. D., Blair, L. A., Needleman, L. A., Gonzales, J. D., Chen, Y., Li, M., Singer, J. D., and Marshall, J. (2006) *J. Biol. Chem.* **281,** 40164–40173
30. Fang, D., Hawke, D., Zheng, Y., Xia, Y., Meisenhelder, J., Nika, H., Mills, G. B., Kobayashi, R., Hunter, T., and Lu, Z. (2007) *J. Biol. Chem.* **282,** 11221–11229
31. Nishiyama, K., Takaji, K., Uchijima, Y., Kurihara, Y., Asano, T., Yoshimura, M., Ogawa, H., and Kurihara, H. (2007) *J. Biol. Chem.* **282,** 17200–17209
32. Sheng, T., Chi, S., Zhang, X., and Xie, J. (2006) *J. Biol. Chem.* **281,** 9–12
33. Li, X., Huston, E., Lynch, M. J., Houslay, M. D., and Baillie, G. S. (2006) *Biochem. J.* **394,** 427–435
34. Burnatowska-Hledin, M., Capps, B., Folta, V., Zhao, P., Mungall, C., Sharangpani, A. M., and Listenberger, L. (2000) *Am. J. Physiol.* (*Cell*) **279,** C266–C273
35. Papadimitriou, E., Unsworth, B. R., Maragoudakis, M. E., and Lelkes, P. I. (1993) *Endothelium* **1,** 207–219
36. Burnatowska-Hledin Zeneberg, A., Roulo, A., Grobe, J., Zhao, P., Lelkes, P. I., Clare, P., and Barney, C. (2001) *Endothelium* **8,** 49–63
37. Goyal, P., Pandey, D., Behring, A., and Siess, W. (2005) *J. Biol. Chem.* **280,** 27569–27577
38. Tang, S., Morgan, K. G., Parker, C., and Ware, J. A. (1997) *J. Biol. Chem.* **272,** 28704–28711
39. Zacchi, P., Gostissa, M., Uchida, T., Salvagno, C., Avolio, F., Volinia, S., Ronai, Z., Blandino, G., Schneider, C., and Del Sal, G. (2002) *Nature* **419,** 853–857
40. Dancey, J., and Sausville, E. A. (2003) *Nat. Rev. Drug. Discov.* **2,** 296–313
41. Yoshiji, H., Kuriyama, S., Ways, D. K., Yoshii, J., Miyamoto, Y., Kawata, M., Ikenaka, Y., Tsujinoue, H., Nakatani, T., Shibuya, M., and Fukui, H. (1999) *Cancer Res.* **59,** 4413–4418
42. Alappat, E. C., Volkland, J., and Peter, M. E. (2003) *J. Biol. Chem.* **278,** 41585–41588
43. Shimada, K., Matsuyoshi, S., Nakamura, M., Ishida, E., and Konishi, N. (2005) *J. Pathol.* **206,** 423–432

44. Luo, K., Ehrlich, E., Xiao, Z., Zhang, W., Ketner, G., and Yu, X. F. (2007) *FASEB J.* **21,** 1742–1750
45. Querido, E., Blanchette, P., Yan, Q., Kamura, T., Morrison, M., Boivin, D., Kaelin, W. G., Conaway, R. C., Conaway, J. W., and Branton, P. E. (2001) *Genes Dev.* **15,** 3104–3117
46. d'Azzo, A., Bongiovanni, A., and Nastasi, T. (2005) *Traffic* **6,** 429–441
47. Soucy, T. A., Smith, P. G., Milhollen, M. A., Berger, A. J., Gavin, J. M., Adhikari, S., Brownell, J. E., Burke, K. E., Cardin, D. P., Critchley, S., Cullis, C. A., Doucette, A., Garnsey, J. J., Gaulin, J. L., Gershman, R. E., Lublinsky, A. R., McDonald, A., Mizutani, H., Narayanan, U., Olhava, E. J., Peluso, S., Rezaei, M., Sintchak, M. D., Talreja, T., Thomas, M. P., Traore, T., Vyskocil, S., Weatherhead, G. S., Yu, J., Zhang, J., Dick, L. R., Claiborne, C. F., Rolfe, M., Bolen, J. B., and Langston, S. P. (2009) *Nature* **458,** 732–736